Cell cycle inhibition provides neuroprotection and reduces glial proliferation and scar formation after traumatic brain injury

Simone Di Giovanni*†, Vilen Movsesyan*†, Farid Ahmed*†, Ibolja Cernak*, Sergio Schinelli‡, Bogdan Stoica*, and Alan I. Faden*§

*Department of Neuroscience, Georgetown University School of Medicine, 3900 Reservoir Road NW, Washington, DC 20057; and ‡Dipartimento di Farmacologia Sperimentale ed Applicata, Facoltà di Farmacia, Università di Pavia, Viale Taramelli 14, 27100 Pavia, Italy

Edited by L. L. Iversen, University of Oxford, Oxford, United Kingdom, and approved April 14, 2005 (received for review February 9, 2005)

Traumatic brain injury (TBI) causes neuronal apoptosis, inflammation, and reactive astrogliosis, which contribute to secondary tissue loss, impaired regeneration, and associated functional disabilities. Here, we show that up-regulation of cell cycle components is associated with caspase-mediated neuronal apoptosis and glial proliferation after TBI in rats. In primary neuronal and astrocyte cultures, cell cycle inhibition (including the cyclin-dependent kinase inhibitors flavopiridol, roscovitine, and olomoucine) reduced up-regulation of cell cycle proteins, limited neuronal cell death after etoposide-induced DNA damage, and attenuated astrocyte proliferation. After TBI in rats, flavopiridol reduced cyclin D1 expression in neurons and glia in ipsilateral cortex and hippocampus. Treatment also decreased neuronal cell death and lesion volume, reduced astroglial scar formation and microglial activation, and improved motor and cognitive recovery. The ability of cell cycle inhibition to decrease both neuronal cell death and reactive gliosis after experimental TBI suggests that this treatment approach may be useful clinically.

flavopiridol | glial scar | neuron | trauma

Traumatic brain injury (TBI) induces secondary molecular changes that lead to neuronal death, microglial activation, inflammation, and reactive astrogliosis. Collectively, these alterations contribute to tissue loss, as well as to glial scar formation that may serve to impair recovery (1, 2). Neuronal apoptosis is an important mechanism of cell death in many models of acute and chronic neurodegeneration. Both caspase-dependent and independent apoptotic pathways have been identified in CNS trauma, although the former has received the most attention (1, 3–7).

Other pathways also play a role in cell death after CNS injury, including activation of proteases (calpains and cathepsins) (8, 9), the mitogen-activated protein kinase (MAPK)-signaling cascade (10, 11), and cell cycle progression (12–14) among others. Cell cycle induction leading to apoptotic neuronal death has been described *in vitro* (15–20) and *in vivo*, including animal models of stroke, amyotrophic lateral sclerosis, and Alzheimer's disease (12, 21–25). Although aberrant cell cycle activation can lead to apoptosis in postmitotic cells, cell cycle transition can also induce proliferation in mitotic cells such as astrocytes and microglia after brain ischemia (26, 27). Activation of such cells is responsible for reactive gliosis, characterized by hyperplasia, hypertrophy, and increase in glial fibrillary acidic protein (GFAP) immunostaining. Reactive gliosis is observed after CNS injuries, including ischemia and trauma. Although microglia and astrocytes secrete important growth factors for neurons, their role after CNS injury seems detrimental for neuronal survival and regeneration (28–31).

Using Affymetrix (Santa Clara, CA) microarrays, we found induction of genes signaling DNA damage and progression of cell cycle following fluid percussion (FP)-induced TBI. Protein expression for these genes was localized in neurons, particularly in those showing expression of caspase 3, as well as in proliferating astrocytes and microglia. In etoposide-treated neuronal cell cultures, cell cycle inhibitors reduced cell cycle protein expression, reduced caspase-mediated apoptosis, and impaired astrocyte proliferation after serum stimulation in culture. Following TBI, flavopiridol reduced neuronal apoptosis, reduced astroglial scar formation, decreased lesion volume, and significantly improved motor and cognitive performance.

Materials and Methods

Rat Lateral FP Trauma Model. Male Sprague–Dawley rats (400 ± 25 g) were anesthetized with sodium pentobarbital (60 mg/kg i.p.). Brain temperature was assessed through a thermister in the temporalis muscle, and body temperature was maintained at 36–37°C. Trauma was induced as described (32). Sham rats (four rats at the 4-h time point and two rats per time point at 8, 24, and 72 h) were subjected to anesthesia and surgery but were not injured. Three unanesthetized, uninjured rats served as naive controls.

Expression Profiling. Tissue from one rat was used for each expression-profiling experiment. Brain tissue was homogenized, RNA was extracted with TRIzol, and expression profiling was performed as described (32, 33) by using rat U34A high-density oligonucleotide microarrays (Affymetrix). Between two and four animals were studied per time point, at 0, 4, 24, and 72 h for each experimental group, including sham and injured.

Microarray Quality Control and Data Analysis. Each microarray underwent a stringent quality control evaluation as described (32, 33). Such data analysis retained the probe sets with the most reliable and consistent performance between multiple measurements among arrays of the same experimental group. Experiment normalization and statistical analysis were performed by using GENESPRING 5.0 software (Silicon Genetics, Redwood, CA) as described (34). We selected for detailed functional analyses only those transcripts that showed a Welch ANOVA t test P value <0.05 and a fold change of at least 1.5 between sham and injured animals for each time point. Functional analysis used the GENESPRING gene ontology tool, DAVID, and GENEMAPP (34).

Semiquantitative RT-PCR. One microgram of total RNA was used for cDNA synthesis by using SuperScript reverse transcriptase and oligo(dT)-primer (Invitrogen). The amount of synthesized cDNA was evaluated by PCR by using primers specific for ribosomal protein RPL19. PCRs were performed as described (32).

This paper was submitted directly (Track II) to the PNAS office.

Abbreviations: FP, fluid percussion; TBI, traumatic brain injury; GFAP, glial fibrillary acidic protein; GADD45, growth arrest and DNA damage inducible protein 45; CDK, cyclin-dependent kinase; PCNA, proliferating cell nuclear antigen; LDH, lactate dehydrogenase; i.c.v., intracerebroventricularly.

†S.D.G., V.M., and F.A. contributed equally to this work.

§To whom correspondence should be addressed. E-mail: fadena@georgetown.edu.

Immunoblotting. Proteins from both frozen rat spinal cord tissues and cultured rat cortical neurons and astrocytes were processed for immunoblotting by standard procedures (see *Supporting Materials and Methods*, which is published as supporting information on the PNAS web site).

Immunocytochemistry. Immunocytochemistry from three injured and two sham animals was performed at 24 h, 72 h, and 28 days. Frozen 12-μm cerebral cortex sections from three injured and two sham animals were incubated under the same coverslip and processed for immunocytochemistry following standard procedures (see *Supporting Materials and Methods*).

Cell Culture. ***Rat primary cortical neurons.*** Cortical neuronal cultures were derived from rat embryonic cortices. Cortices from 15- to 16-day-old embryos were cleaned from their meninges and blood vessels, minced, and dissociated as described (9). More information is available in *Supporting Materials and Methods*.
Rat primary astrocytes. Purified astrocyte cultures were prepared from 20-day-old Sprague–Dawley rat embryos. Cortices were dissected and then mechanically dissociated as described (35). The cultures comprise >95% GFAP-positive cells (35). For detailed information, see *Supporting Materials and Methods*.

MRI. At 21 days after injury, animals were examined by using a Bruker (Billerica, MA) 7.0-tesla spectrometer/imager, as described (9). Lesion volumes were estimated from the summation of areas of hyperintensity in cerebrum multiplied by slice thickness by using Bruker PARAVISION 2.1 imaging software.

Motor Function Assessment. Motor function was evaluated by using standardized motor scoring, i.e., composite neuroscore on days 1, 2, 3, 7, 14, 15, 16, and 17 posttrauma as described (36). Tests included the ability to maintain position on an inclined plane in two vertical and two horizontal positions, forelimb flexion, and forced lateral pulsion; composite neurological scores range from 0 to 35.

Cognitive Function Assessment. Spatial learning was tested by using the Morris water maze, as described (36). A series of 16 training trials administered in blocks of 4 with an intertribal interval of 30 min were conducted on days 14 to 17 postinjury. To control for motor impairment, animals were tested to locate a visible platform at least 2 h after the last training trial.

Drugs. Flavopiridol was provided by the Developmental Therapeutics Program, Division of Cancer Treatment and Diagnosis, National Cancer Institute, National Institutes of Heath; roscovitine and olomoucine were purchased from Calbiochem; etoposide was obtained from Sigma.

Results

DNA Damage and Cell Cycle-Related Genes Are Induced After Brain Trauma. To investigate potential molecular factors involved in secondary injury after TBI, we used Affymetrix high-density oligonucleotide microarrays. We generated a list of significantly altered genes, including those profiles with at least 40% of "present" P calls, a fold change of 1.5, and a Welch ANOVA *t* test *P* value <0.05 between sham and injured samples for each time point (for complete gene list, see ref. 32). We found significantly increased expression for a number of DNA damage-related and cell cycle genes, including growth arrest and DNA damage inducible protein 45 (GADD45), c-MYC, cyclin D1, cdk-4, E2F-5, and proliferating cell nuclear antigen (PCNA) between 4 and 72 h (Fig. 1 *a* and *b*). In contrast, cell cycle inhibitor genes were either unchanged (p21) or significantly down-regulated (p27) at the same time points (data not shown).

To validate these expression-profiling data, we performed RT-PCR in parallel rat sham and injured samples (0, 4, 8, 24, and 72 h); these data confirmed microarray mRNA expression changes for GADD45α, c-MYC, PCNA, and p27 (Fig. 1*c*).

Immunoblotting was also performed to quantify protein expression in both sham and injured animals at representative time points after injury (24 and 72 h) (Fig. 1 *d* and *e*). Increased expression for GADD45α, PCNA, and cyclin D1 and down-regulation for p27 were found in injured brains compared with shams (Fig. 1 *d* and *e*), which paralleled mRNA expression changes.

Cyclin-Dependent Kinase (CDK) Inhibitors Reduce Cell Death in Etoposide-Treated Primary Cortical Neurons. In parallel studies, we examined the effects of the DNA-damaging and proapoptotic agent etoposide on cell cycle induction and apoptosis in rat primary cortical neurons. We treated cultures with etoposide (50 μM) to induce DNA damage and cell death and tested the effect of the CDK/cell cycle inhibitors flavopiridol, roscovitine, or olomoucine on neuronal survival. All these compounds are selective CDK inhibitors, although they have somewhat different affinity and selectivity for specific CDKs and inhibit the G_1-S and G_2-M transition phases of the cell cycle (37, 38). Cell viability [lactate dehydrogenase (LDH) release] and degree of apoptotic cell death (cells with Hoescht-positive nuclei) were evaluated 24 h after treatment. In addition, protein levels for cyclin D1, PCNA, and p27 were measured by immunoblotting. Etoposide significantly reduced cell viability as reflected by LDH release (250% increase) (Fig. 2*a*) and significantly induced apoptotic nuclear condensation resulting in 225% increase in cells with apoptotic nuclei (Hoechst-positive) (Fig. 2*b*). Flavopiridol at 1-, 10-, or 100-μM concentrations significantly reduced LDH release (from 250% to 120%) as well as the number of apoptotic cells (225% to 135%, Fig. 2 *a* and *b*). Administration of roscovitine or olomoucine in parallel experiments also reduced LDH release and neuronal apoptosis after etoposide treatment. Roscovitine or olomoucine caused 22% and 51% reduction of etoposide-induced LDH release, respectively. Immunoblotting showed increased expression of cyclin D1 and PCNA after etoposide, which was inhibited when flavopiridol was added 1 hour before etoposide administration (Fig. 2*c*). In contrast, expression of the endogenous CDK inhibitor p27 was strongly inhibited by etoposide and was reversed by flavopiridol treatment (Fig. 2*c*). Active caspase 3 was strongly induced by etoposide but reversed after flavopiridol treatment (Fig. 2*c*). This result suggests that inhibition of aberrant cell cycle progression plays a role in neuronal survival after DNA damage in cortical neurons.

CDK Inhibitors Reduce Proliferation of Primary Cortical Astrocytes. We also examined the effects of flavopiridol or roscovitine on astrocyte proliferation *in vitro*. Rat brain astrocytes were dissected and put in culture according to standard procedures as described (35). Proliferation was induced with 24 h of serum stimulation (10% FBS). Drugs were added to either serum-treated or nontreated (baseline samples) cells at different concentrations: flavopiridol at 100 nM, 1 μM, and 10 μM or roscovitine at 1 μM, 10 μM, and 100 μM for 48 h. Cell viability assay (Cell Titer 96 Aqueous One Solution Cell Proliferation Assay, Promega) was used to measure modulation of cell proliferation after serum alone versus serum plus flavopiridol treatment. Flavopiridol or roscovitine reduced cell proliferation in a concentration-dependent manner (Fig. 2*d*), although, flavopiridol was far more effective. Cell numbers after 10 μM flavopiridol were comparable with nonstimulated cells, showing that the drug entirely blocked proliferation of astrocytes (Fig. 2*d*). Flavopiridol treatment also completely attenuated cyclin D1 and PCNA protein expression after FBS, as shown by immunoblotting (Fig. 2*e*). In parallel experiments, cells were collected for cell cycle profile analysis by using FACS cell sorting. Importantly, S phase was increased by 224% after serum stimulation, compared with baseline, and restored to baseline levels after flavopiridol treatment (10 μM) (Fig. 2*f*). No evidence of cell death was found

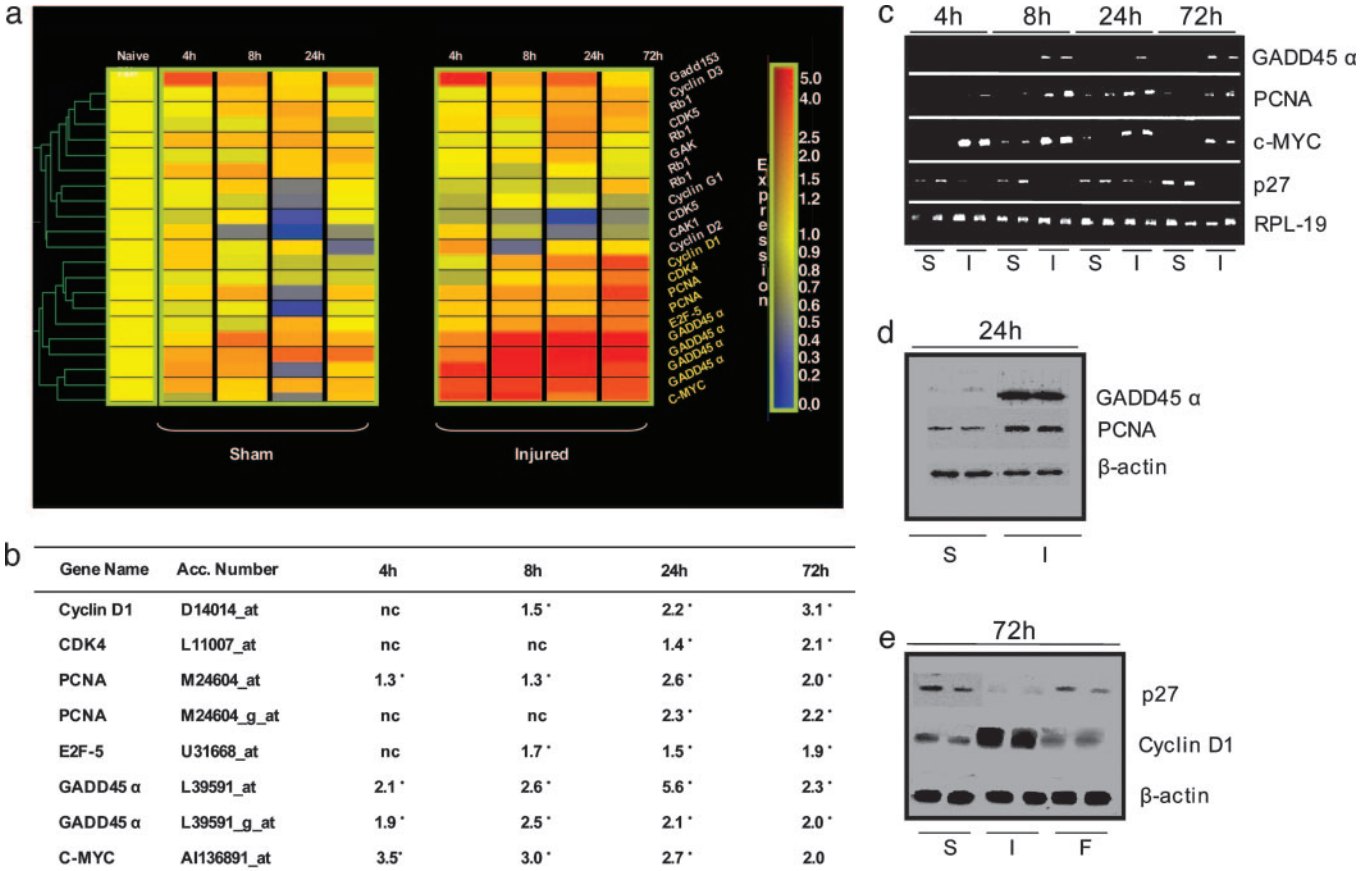

b

Gene Name	Acc. Number	4h	8h	24h	72h
Cyclin D1	D14014_at	nc	1.5 *	2.2 *	3.1 *
CDK4	L11007_at	nc	nc	1.4 *	2.1 *
PCNA	M24604_at	1.3 *	1.3 *	2.6 *	2.0 *
PCNA	M24604_g_at	nc	nc	2.3 *	2.2 *
E2F-5	U31668_at	nc	1.7 *	1.5 *	1.9 *
GADD45 α	L39591_at	2.1 *	2.6 *	5.6 *	2.3 *
GADD45 α	L39591_g_at	1.9 *	2.5 *	2.1 *	2.0 *
C-MYC	AI136891_at	3.5*	3.0 *	2.7 *	2.0

Fig. 1. Cell cycle and DNA damage-related mRNA and protein changes after TBI. (*a*) Shown is a dendrogram (gene tree) obtained nucleating altered transcripts between sham and injured brains. Bar graph (*Right*) shows the color code for gene expression levels from low (blue) to high (red). These transcripts are up-regulated between 4 and 72 h after TBI (gene names in yellow indicate a Welch *t* test *P value* <0.05 between sham and injured at one corresponding time point). (*b*) Table shows gene name, accession number, and quantitation (fold changes) of mRNA changes by Affymetrix for the transcripts represented in the dendrogram. Genes with asterisks indicate a Welch *t* test *P* value <0.05 between sham and injured at the corresponding time point. (*c*) RT-PCR confirms expression of mRNAs for GADD45, PCNA, c-Myc, and p27 (ribosomal protein L-19 was used as control). (*d*) Immunoblots show increased GADD45 and PCNA protein levels in injured (I), versus sham (S) brains at 24 h in two parallel experiments. β-Actin is a loading control. (*e*) Immunoblotting at 72 h shows induction of cyclin D1 and inhibition of p27 protein expression after TBI in injured (I) versus sham (S) brains; flavopiridol (F) rescues p27 expression and inhibits cyclin D1. β-Actin is a loading control.

in astrocytes after flavopiridol treatment (data not shown), as measured by Hoechst staining.

Flavopiridol Reduces Neuronal Cell Death, Microglial Activation, Astroglial Proliferation, and Scar Formation After TBI. To evaluate the effect of flavopiridol *in vivo* on neuronal death and glial proliferation through modulation of cell cycle, we performed immunoblotting and immunocytochemistry experiments after TBI in rats, comparing brains from animals treated by intraventricular delivery of flavopiridol or vehicle. Immunoblotting comparing cortex from shams, vehicle-treated rats, and flavopiridol-treated rats at 72 h posttrauma showed that cyclin D1 expression was induced after TBI and strongly inhibited by flavopiridol, whereas p27 expression was inhibited after injury and normalized after treatment (Fig. 1*e*). Immunohistochemistry was performed in sham, vehicle, and flavopiridol-treated rats at 24 and 72 h. Double- and triple-labeling experiments were done with either neuronal-specific marker NeuN, astrocyte marker GFAP, or activated microglia marker OX-42, together with cyclin D1 and/or activated caspase 3.

Trauma increased expression of cyclin D1 in neurons, microglia, and astrocytes at 24 and 72 h. Cell counting was performed in both cortex and hippocampus at 72 h, and 13.3 ± 1.7% of neurons showed expression of cyclin D1 in cortex around the injury site compared with 6.6 ± 1.3% in the contralateral cortex of vehicle-treated animals. Cyclin D1-positive neurons were reduced to 5.5 ± 0.9% after flavopiridol in the injury region area (Fig. 3*a*); 82 ± 3.2% of neurons expressing cyclin D1 after injury were also positive for active caspase 3, compared with 5.4 ± 1.6% in the contralateral cortex, and to 11.6 ± 1.9% after flavopiridol (Fig. 3*b*). In the ipsilateral hippocampus, 10.5 ± 1.1% of neurons were cyclin D1-positive compared with 2.7 ± 0.4% on the contralateral side in vehicle-treated animals and 2.3 ± 0.6% in flavopiridol-treated animals ipsilaterally (Fig. 6*a*, which is published as supporting information on the PNAS web site). Moreover, 75 ± 3.8% cyclin D1-positive neurons after injury were also positive for caspase 3, whereas only rare active caspase 3 and cyclin D1-positive cells were detected in the contralateral side, and after flavopiridol (Fig. 6*b*). Astrocyte proliferation was observed in the cortex around the injury site after trauma as an increase in number of GFAP-positive cells. Astrocytes positive for cyclin D1 and PCNA were also increased at both 24 and 72 h. GFAP-positive cells increased by 83 ± 4.1% in the injured cortex compared with the controlateral region. We found that 85.5 ± 4.7% GFAP-positive cells around the injury site were also positive for cyclin D1 (Fig. 4*a*). Flavopiridol treatment limited the increase of GFAP-positive cells around the injury to only 23 ± 3.6% compared with the contralateral cortex (Fig. 4*a*). Cyclin D1 was present only in 35 ± 3.3% GFAP-positive cells around the injury site after flavopiridol treatment (Fig. 4*a*). A 45 ± 4.3% increase in GFAP-positive cells occurred in the ipsilateral hippocampus compared with the contralateral side in vehicle-

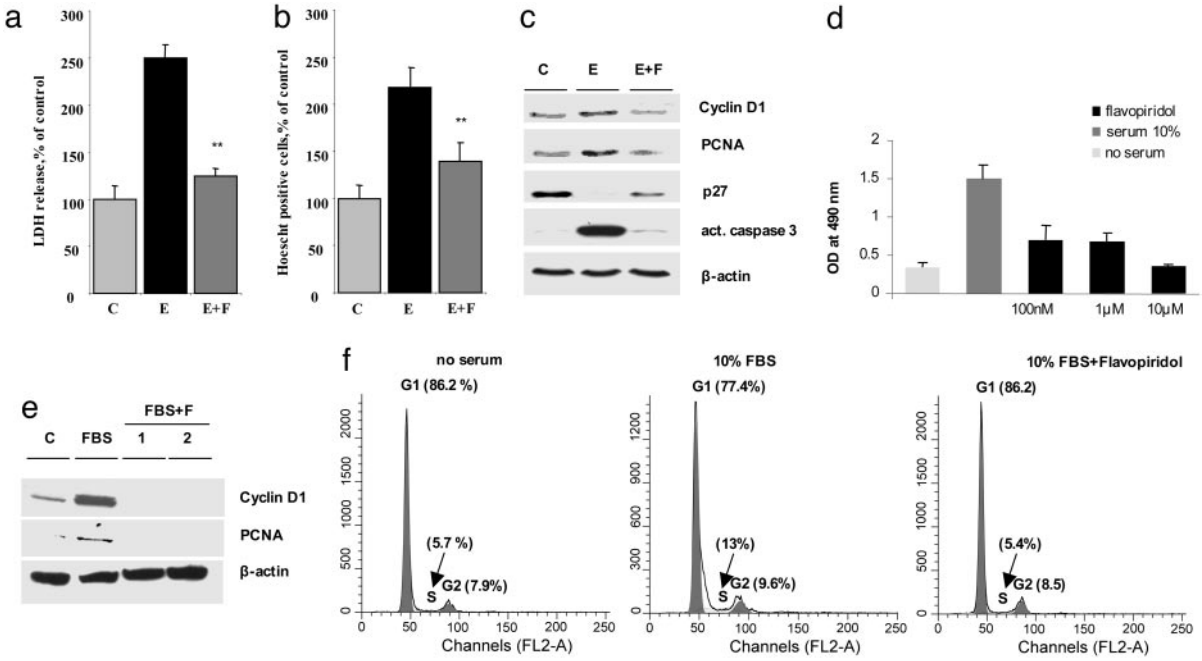

Fig. 2. Flavopiridol promotes neuronal survival after DNA damage and inhibits astrocyte proliferation by blocking cell cycle proteins and cell cycle progression. (*a* and *b*) Flavopiridol treatment protects cells from death induced by etoposide (LDH release) (*a*) and number of Hoechst-positive cells (*b*) in primary cortical neurons at 24 h. (*c*) Immunoblotting shows expression of cell cycle proteins and caspase 3 after etoposide treatment, and etoposide plus flavopiridol treatment from rat cortical neuronal cells after treatment with etoposide (lane E) and after etoposide plus flavopiridol (lane E+F) at 24 h. (*d*) Flavopiridol blocks proliferation of cultured rat astrocytes. Shown are data from MTT cell viability assay in astrocytes after serum stimulation and treatment with flavopiridol. Values on *y* axis are expressed in OD, reflecting number of viable cells. (*e*) Flavopiridol completely suppresses cyclin D1 and PCNA protein expression in proliferating astrocytes. Immunoblotting at 48 h after serum stimulation (lane FBS) shows induction of cyclin D1 and PCNA compared with control resting astrocytes (lane C). Flavopiridol in duplicate experiments, administered 1 h before FBS completely suppresses cyclin D1 and PCNA protein expression (lanes FBS+F). (*f*) Flavopiridol reduces S phase in proliferating astrocytes to basal levels (FACS).

treated animals. We found that 11 ± 1.1% GFAP-positive cells were also cyclin D1-positive, whereas, after flavopiridol, there was only a 20.5 ± 5.1% increase in GFAP-positive cells in the hippocampus, and only 2 ± 0.2% were also cyclin D1-positive (Fig. 4*b*). There was a strong increase in immunoreactivity for active microglia marker OX-42 in the cortex around the injury site after injury, whereas no active microglia were detected in the controlateral cortex: 82 ± 5.2% of OX-42-positive cells were also cyclin D1-positive (Fig. 4*c*) and PCNA-positive (data not shown). Flavopiridol treatment reduced the number of activated microglia to 30 ± 3.6% compared with the vehicle-treated animals, and only rare cyclin D1-positive cells were found (Fig. 4*c*).

At 28 days post-trauma, the injured cortex was compared between vehicle and flavopiridol-treated animals. Brains were immunostained with GFAP antibody for astroglia and TOPRO nuclear staining. Less tissue loss was evident at the injury site in the flavopiridol-treated animals versus vehicle (Fig. 4*d*), with the rim of GFAP-positive cells around the central area of tissue loss markedly reduced. Given the near absence of a defined lesion in the flavopiridol-treated animals, in contrast to controls, quantitative com-

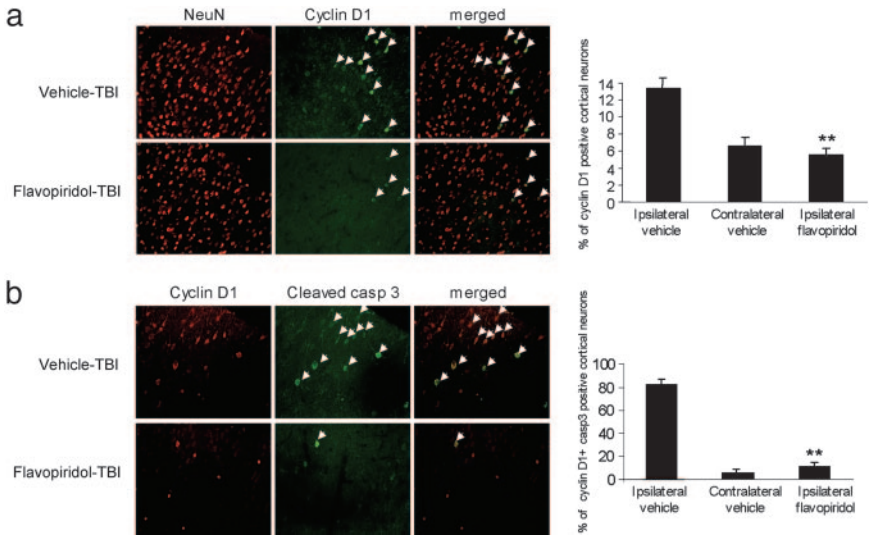

Fig. 3. Immunofluorescence shows the expression of cyclin D1 and active caspase 3 in cortical neurons after TBI, and effects of flavopiridol treatment. (*a*) Double immunofluorescence in coronal sections of the brain cortex around the injury site shows staining for cyclin D1 in vehicle, and flavopiridol-treated animal after TBI, and for the neuronal marker NeuN. Cyclin D1 expression is induced in cortical neurons after TBI and strongly reduced after flavopiridol compared with vehicle (arrows). (Original magnification: ×125.) Bar graphs show quantitation of cortical neurons expressing cyclin D1 in ipsilateral and contralateral cortex in vehicle-treated rats, compared with flavopiridol (ipsilateral) (**, $P < 0.01$). (*b*) Double immunofluorescence in coronal sections of the brain cortex around the injury site shows staining for cyclin D1 in vehicle, and flavopiridol-treated animal after TBI, and for active caspase 3. Flavopiridol strongly reduces cyclin D1-positive and active caspase 3-positive neurons (arrows). (Original magnification: ×125.) Bar graphs show quantitation of cortical neurons coexpressing cyclin D1 and cleaved caspase 3 in ipsilateral and contralateral cortex in vehicle-treated rats, compared with flavopiridol (ipsilateral) (**, $P < 0.01$).

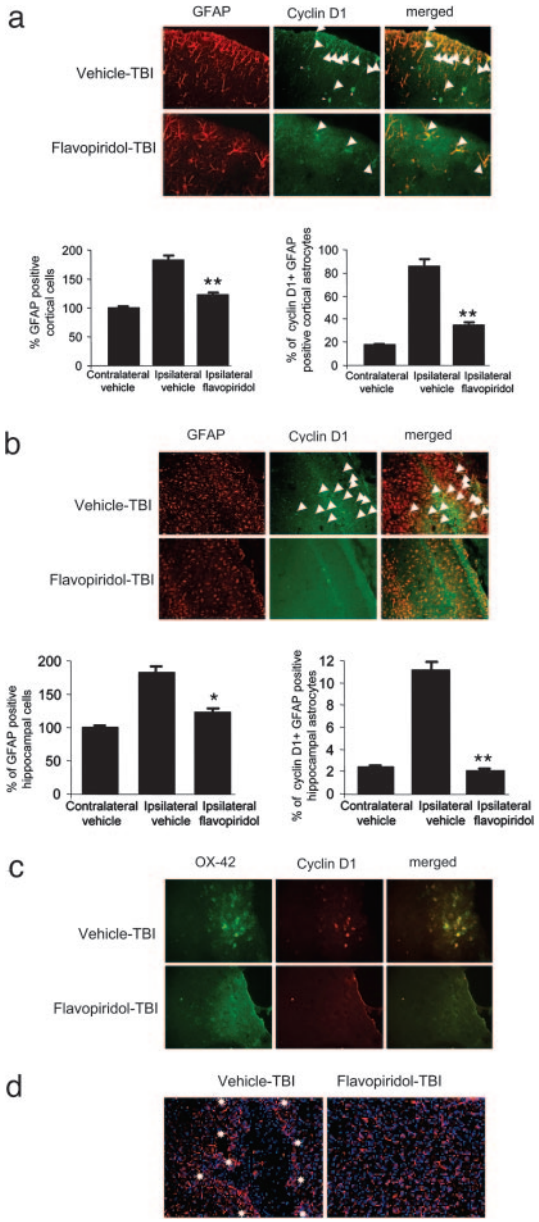

Fig. 4. Immunofluorescence in glial cells after TBI and flavopiridol treatment. (*a*) Double immunofluorescence in coronal sections of brain cortex around the injury site shows staining for cyclin D1 and for astrocyte marker GFAP in vehicle, and flavopiridol-treated animals after TBI. Strong reduction of cyclin D1-positive and GFAP-positive cells is present after flavopiridol compared with vehicle (arrows). (Original magnification: ×125.) Bar graphs show quantitation of these data (**, $P < 0.01$). (*b*) Double immunofluorescence in coronal sections of hippocampus (CA1 and CA2) on the injury site shows staining for cyclin D1 and GFAP in vehicle, and flavopiridol-treated animal after TBI. Strong reduction of cyclin D1-positive and GFAP-positive cells is present after flavopiridol compared with vehicle (arrows). (Original magnification: ×125.) Bar graphs show quantitation of these data (*, $P < 0.05$; **, $P < 0.01$). (*c*) Double immunofluorescence in coronal sections of brain cortex around the injury site shows staining for cyclin D1 and for activated microglia marker OX-42 in vehicle, and flavopiridol-treated animals after TBI. Just sporadic GFAP-positive cells are present after flavopiridol (arrows). (Original magnification: ×125.) (*d*) Immunostaining for GFAP and nuclear marker (TOPRO) in ipsilateral cortex after TBI, comparing vehicle and flavopiridol-treated rats at 28 days posttrauma. Flavopiridol (250 μM) limits the injury-induced reactive gliosis and tissue loss. (Original magnification: ×125.)

parisons of the scar volume *per se* was not feasible. However, lesion differences between treated and control animals, as observed by histology, paralleled reductions in lesion volume observed by MRI.

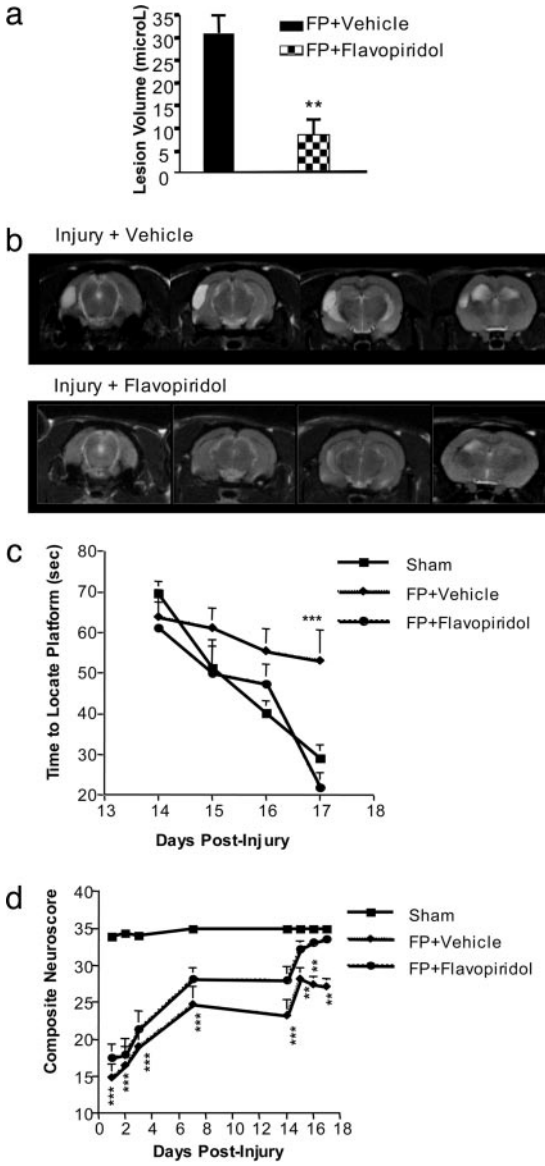

Fig. 5. Flavopiridol significantly reduces lesion volume 21 days after TBI in rats. (*a*) Bar graph shows significant reduction of lesion volume 21 days after TBI (30 min after the injury, at 250 μmol i.c.v.; $n = 7$; lesion volumes: mean ± SEM); (**, $P < 0.01$ vs. FP plus vehicle). (*b*) Representative T_2-weighted MRI of vehicle and flavopiridol-treated rats shows marked reduction of lesion volume. (*c*) Flavopiridol improves cognitive performance as measured by the Morris water maze test (***, $P < 0.001$ compared with sham control animals). (*d*) Flavopiridol restores motor function close to control levels. Results are shown as daily mean ± SEM (**, $P < 0.01$ and ***, $P < 0.001$ vs. sham controls).

Flavopiridol Reduces Lesion Volume and Favors Functional Recovery *in Vivo* After TBI. To further address whether inhibition of cell cycle-related proteins reduces the lesion volume after TBI, we administered 250 μM flavopiridol intracerebroventricularly (i.c.v.) 30 min after injury, and performed T2-weighted MRI 21 days after trauma. A marked and significant reduction of brain lesion volume was found in flavopiridol-treated injured animals as compared with vehicle controls (Fig. 5 *a* and *b*). We also examined the effects of flavopiridol administration on trauma-induced cognitive deficits, measured by Morris water maze test; flavopiridol treatment prevented the injury-induced cognitive deficit (Fig. 5*c*). Moreover, flavopiridol-treated animals recovered motor function to levels similar to those of uninjured controls (Fig. 5*d*), in contrast to vehicle-treated animals that remained substantially impaired.

Discussion

Our data show that activation of cell cycle proteins after TBI is associated with cell death and caspase activation in neurons, but with proliferation of astrocytes and microglia. Moreover, cell cycle inhibition by flavopiridol treatment reduces neuronal cell death, as well as astroglial and microglial proliferation. Importantly, these changes were paralleled by a remarkable reduction in lesion volume and by nearly complete functional recovery.

These data are consistent with the hypothesis that activation of cell cycle proteins in postmitotic cells, such as neurons, triggers an aberrant cell cycle reentry mechanism that leads to cell death (12–14). *In vivo* studies of cortical or spinal cord neurons after ischemia or excitotoxic-mediated DNA damage have shown the occurrence of apoptotic cell death associated with cyclin D1-cdk4, cyclin G, PCNA, or Rb/E2F protein and mRNA overexpression (21–25). Inhibition of neuronal death, and improvement of functional recovery with flavopiridol treatment has been reported after brain ischemia in rats, although effects on glial and microglial cells were not addressed (39, 40). We have also recently shown that similar changes in cell cycle genes occur 24 h after experimental spinal cord injury and were expressed in neurons showing signs of DNA damage and apoptotic cell death (33). Thus, expression of cell cycle proteins may reflect DNA damage, attempted repair, and subsequent apoptosis of injured neurons under diverse experimental conditions.

Cell cycle inhibitors, including flavopiridol, have been shown to protect injured primary neurons from cell death by blocking proteins involved in the G_1/S phase of cell cycle (41, 42). We induced DNA damage and examined cell cycle induction in cultured primary cortical neurons. Administration of etoposide caused caspase-associated neuronal apoptosis at 24 h, accompanied by induction of cyclin D1 and PCNA and the reduction of p27. Moreover, cell cycle inhibition significantly reduced cell death, inhibited protein expression of cyclin D1 and PCNA, and enhanced p27 expression. Cell cycle inhibitors also effectively blocked glial proliferation *in vitro*. Taken together, these data suggest that cell cycle inhibition after DNA damage and aberrant cell cycle reentry reduces caspase-mediated neuronal apoptosis and may inhibit proliferation of mitotic cells such as astroglia or microglia.

After TBI, flavopiridol treatment reduced the expression of cell cycle proteins in neurons and glia, decreased neuronal apoptosis and caspase expression in ipsilateral cortex and hippocampus, and limited microglial and astroglial proliferation after injury. These changes were associated with remarkable improvement in tissue preservation and behavioral outcome. This striking degree of neuroprotection likely reflects the multifactorial actions of this drug class: attenuating posttraumatic neuronal cell loss; reducing the induction of reactive microglia with the likely related decrease of microglial-associated inflammatory factors; and limiting astroglial proliferation and the associated glial scar, with potential reduction of glial-induced inhibitors of regeneration/plasticity. It should be emphasized that cell death was not induced in nonproliferating glial cells by flavopiridol, suggesting that cell cycle inhibition does not affect "physiological" levels of astroglia, which may be important for support and production of trophic factors in the CNS. Moreover, it is likely that early inhibition of proliferating reactive astrocytes and microglia would impair production and later accumulation of molecules (such as proteoglycans) involved in glial scar formation.

Flavopiridol has been tested in phase I and II clinical trials as a potential antineoplastic agent, including leukemias/lymphomas, non-small-cell lung cancer, non-Hodgkin lymphoma, and prostate, colon, gastric, and kidney carcinomas (37, 38). Although it has not proved effective as a clinical anti-cancer agent to date, it has largely proved to be safe at doses needed to block induction of cell cycle proteins in animal models. Possible use of cell cycle inhibitors for treatment of stroke or trauma would only require acute or subacute administration, thereby further reducing potential toxicity. We conclude that use of cell cycle inhibitors may provide an effective therapeutic target for the treatment of CNS trauma because of their multimodal actions, which include inhibition of neuronal cell death, the posttraumatic inflammatory response, and glial scar formation.

We thank Idalia Cruz, Elvira Dabaghyan, Lioudmila Zoubak, and Jeanette Beers for technical assistance. This work was supported by National Institutes of Health (NIH) Grant NS 36537-03 and Contract NIH-NINDS-01 (NS-1-2339) (to A.I.F.) and NIH Grant HD4-0677.

1. Raghupathi, R. (2004) *Brain Pathol.* **14,** 215–222.
2. McGraw, J., Hiebert, G. W. & Steeves, J. D. (2001) *J. Neurosci. Res.* **63,** 109–115.
3. Yakovlev, A. G. & Faden, A. I. (2001) *Mol. Neurobiol.* **24,** 131–144.
4. Liou, A. K., Clark, R. S., Henshall, D. C., Yin, X. M. & Chen, J. T. (2003) *Prog. Neurobiol.* **69,** 103–142.
5. Faden, A. I. (2002) *Curr. Opin. Neurol.* **15,** 707–712.
6. Lotocki, G., Alonso, O. F., Frydel, B., Dietrich, W. D. & Keane, R. W. (2003) *J. Cereb. Blood Flow Metab.* **23,** 1129–1136.
7. Frantseva, M., Perez-Velazquez, J. L., Tonkikh, A., Adamchik, Y. & Carlen, P. L. (2002) *Prog. Brain Res.* **137,** 171–176.
8. Ray, S. K. & Banik, N. L. (2003) *Curr. Drug Targets CNS Neurol. Disord.* **2,** 173–189.
9. Knoblach, S. M., Alroy, D. A., Nikolaeva, M., Cernak, I, Stoica, B. A. & Faden, A. I. (2004) *J. Cereb. Blood Flow Metab.* **24,** 1119–1132.
10. Kuan, C. Y., Whitmarsh, A. J., Yang, D. D., Liao, G., Schloemer A. J., Dong, C., Bao, J., Banasiak, K. J., Haddad, G. G., Flavell, R. A., Davis, R. J. & Rakic, P. (2003) *Proc. Natl. Acad. Sci. USA* **100,** 15184–15189.
11. Hu, B., Liu, C., Bramlett, H., Sick, T. J., Alonso, O. F., Chen, S & Dietrich, W. D. (2004) *J. Cereb. Blood Flow Metab.* **24,** 934–943.
12. Becker, E. B. & Bonni, A. (2004) *Prog. Neurobiol.* **72,** 1–25.
13. Copani, A., Uberti, D., Sortino, M. A., Bruno, V., Nicoletti, F. & Memo, M. (2001) *Trends Neurosci.* **24,** 25–31.
14. Liu, D. X. & Greene, L. A. (2001) *Cell Tissue Res.* **305,** 217–228.
15. Freeman, R. S., Estus, S. & Johnson, E. M. Jr. (1994) *Neuron* **12,** 343–355.
16. Padmanabhan, J., Park, D. S., Greene, L. A. & Shelanski, M. L. (1999) *J. Neurosci.* **19,** 8747–8756.
17. Kranenburg, O., van der Eb, A. J. & Zantema, A. (1996) *EMBO J.* **15,** 46–54.
18. Boutillier, A. L., Trinh, E. & Loeffler, J. P. (2000) *Oncogene* **19,** 2171–2178.
19. Park, D. S., Morris, E. J., Bremner, R., Keramaris, E., Padmanabhan, J., Rosenbaum, M., Shelanski, M. L., Geller, H. M & Greene L. A. (2000) *J. Neurosci.* **20,** 3104–3114.
20. Herrup, K., Neve, R., Ackerman, S. L. & Copani, A. (2004) *J. Neurosci.* **20,** 9232–9239.
21. Van Lookeren–Campagne, M. & Gill, R. (1998) *Neuroscience* **84,** 1097–1112.
22. Sakurai, M., Hayashi, T., Abe, K., Itoyama, Y., Tabayashi, K. & Rosenblum, W. I. (2000) *Stroke* **31,** 200–207.
23. Ino, H. & Chiba, T. (2001) *J. Neurosci.* **21,** 6086–6094.
24. Xiang, Z., Ho, L., Valdellon, J., Borchelt, D., Kelley, K., Spielman, L., Aisen, P. S. & Pasinetti, G. M. (2002) *Neurobiol. Aging* **23,** 327–334.
25. Nguyen, M. D., Boudreau, M., Kriz, J., Couillard-Despres, S., Kaplan, D. R. & Julien, J. P. (2003) *J. Neurosci.* **23,** 2131–2140.
26. Kato, H., Takahashi, A. & Itoyama, Y. (2003) *Brain Res. Bull.* **60,** 215–221.
27. Koguchi, K., Nakatsuji, Y., Nakayama, K. & Sakoda, S. (2002) *Glia* **37,** 93–104.
28. Fawcett, J. W. (1997) *Cell Tissue Res.* **290,** 371–377.
29. McMillian, M. K., Thai, L., Hong, J. S., O'Callaghan, J. P. & Pennypacker, K. R. (1994) *Trends Neurosci.* **17,** 138–142.
30. Nieto-Sampedro, M. (1999) *Adv. Exp. Med. Biol.* **468,** 207–224.
31. Ridet, J. L., Malhotra, S. K., Privat, A. & Gage, F. H. (1997) *Trends Neurosci.* **20,** 570–577.
32. Natale, J. E., Ahmed, F., Cernak, I., Stoica, B. & Faden, A. I. (2003) *J. Neurotrauma* **20,** 907–927.
33. Di Giovanni, S., Knoblach, S. M., Brandoli, C., Aden, S. A., Hoffman, E. P. & Faden, A. I. (2003) *Ann. Neurol.* **53,** 454–468.
34. Di Giovanni, S., Molon, A., Broccolini, A., Melcon, G., Mirabella, M., Hoffman, E. P. & Servidei, S. (2004) *Ann. Neurol.* **55,** 195–206.
35. Schinelli, S., Zanassi, P., Paolillo, M., Wang, H., Feliciello, A. & Gallo, V. (2001) *J. Neurosci.* **21,** 842–853.
36. Faden, A. I., Knoblach, S. M., Cernak, I., Fan, L., Vink, R., Araldi, G. L., Fricke, S. T., Roth, B. L. & Kozikowski, A. P. N. (2003) *J. Cereb. Blood Flow Metab.* **23,** 342–354.
37. Senderowicz, A. M. (2003) *Oncogene* **22,** 6609–6620.
38. Swanton, C. (2004) *Lancet Oncol.* **5,** 27–36.
39. Osuga, H., Osuga, S., Wang, F., Fetni, R., Hogan, M. J., Slack, R. S., Hakim, A. M., Ikeda, J. E. & Park, D. S. (2000) *Proc. Natl. Acad. Sci. USA* **97,** 10254–10259.
40. Wang, F., Corbett, D., Osuga, H., Osuga, S., Ikeda, J. E., Slack, R. S., Hogan, M. J., Hakim, A. M. & Park, D. S. (2002) *J. Cereb. Blood Flow Metab.* **22,** 171–182.
41. Bartek, J. & Lukas, J. (2001) *FEBS Lett.* **490,** 117–122.
42. Kruman, I. I., Wersto, R. P., Cardozo-Pelaez, F., Smilenov, L., Chan, S. L., Chrest, F. J., Emokpae, R., Jr., Gorospe, M. & Mattson, M. P. (2004) *Neuron* **41,** 549–561.